Acoustic Finite Element Analysis of a Slit Model with Consideration of Air Viscosity

M. Sasajima, M. Watanabe, T. Yamaguchi Y. Kurosawa, Y. Koike

Abstract—In very narrow pathways, the speed of sound propagation and the phase of sound waves change due to the air viscosity. We have developed a new finite element method (FEM) that includes the effects of air viscosity for modeling a narrow sound pathway. This method is developed as an extension of the existing FEM for porous sound-absorbing materials. The numerical calculation results for several three-dimensional slit models using the proposed FEM are validated against existing calculation methods.

Keywords—Simulation, FEM, air viscosity, slit.

I. INTRODUCTION

COMPUTER-AIDED engineering has been used extensively in recent years for acoustic analyses. However, the conventional analysis approach is used predominantly for relatively large structures or large equipment. For example, for a structure with a small volume like a portable electronic device, very few methods of sound propagation analysis are available. The viscosity of air in these narrow pathways results in damping. Consequently, the speed of sound propagation decreases, and a phase delay occurs. Therefore, to carry out accurate acoustic analysis for small electronic devices, we must consider the effect of the air viscosity. This effect is not considered in conventional acoustic analysis. In the present study, we developed a new finite element method (FEM) that includes the effects of air viscosity in narrow places in the sound pathway of small electronic devices. This has been developed as an extension of the acoustic FEM proposed by Yamaguchi [1], [2] for a porous sound-absorbing material. We attempted numerical analysis in the frequency domain with our acoustic solver that uses the proposed FEM [3]-[5].

For the numerical calculations, we used several slit models having a rectangular cross section. Then we compared the proposed FEM with the theoretical analysis and with the generally used finite element analysis that does not include the effects of the viscosity of the air.

M. Sasajima, M. Watanabe, and Y. Koike are with the Strategic Research & Development Division, Foster Electric Co., Ltd., 196-8550, 1-1-109 Tsutsujigaoka, Akishima, Tokyo, Japan (phone: 042-847-3334; e-mail: sasajima@foster.co.jp, mtwatanabe@ foster.co.jp, koike@ foster.co.jp).

T. Yamaguchi is with the Department of Mechanical System Engineering, Gunma University, 376-8515, 1-5-1, Tenjin-cho, Kiryu, Gunma, Japan (e-mail: yamagme3@gunma-u.ac.jp).

Y. Kurosawa is with the Department of Precision Mechanical System Engineering, Teikyo University, 320-8551, 1-1, Toyosatodai, Utsunomiya, Tochigi, Japan (e-mail: ykurosawa@mps.teikyo-u.ac.jp).

II. NUMERICAL PROCEDURES

We have developed a new FEM that incorporates air viscosity at small amplitudes. Fig. 1 shows the direct Cartesian coordinate system and a constant strain element of a three-dimensional (3D) tetrahedron. Here, u_x, u_y, and u_z are the displacements in the x, y, and z directions at arbitrary points in the element. The strain energy $\widetilde{U}$ can be expressed as follows:
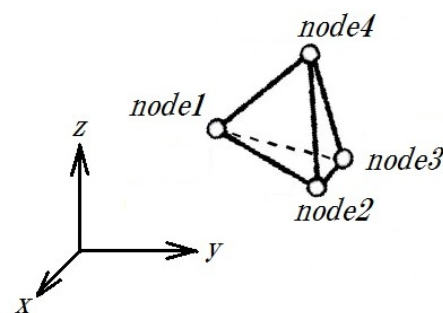

Fig. 1 Direct Cartesian coordinate system and a constant strain element

$$\widetilde{U} = \frac{1}{2} E \iiint_e \left(\frac{\partial u_x}{\partial x} + \frac{\partial u_y}{\partial y} + \frac{\partial u_z}{\partial z} \right)^2 dxdydz \tag{1}$$

where E is the bulk modulus of elasticity of the air. The time derivative of the particle displacement is expressed as $\dot{u}$. Therefore, the kinetic energy $\widetilde{T}$ can be expressed as follows:

$$\widetilde{T} = \frac{1}{2} \iiint_e \rho \{\dot{u}\}^T \{\dot{u}\} dxdydz \tag{2}$$

where ρ is the effective density of the element, and T represents a transposition. The viscosity energy $\widetilde{D}$ of a viscous fluid can be expressed as follows:

$$\widetilde{D} = \iiint_e \frac{1}{2} \{\overline{T}\}^T \{\Gamma\} dxdydz \tag{3}$$

where $\{\overline{T}\}$ is the stress vector attributable to viscosity. The relationship between the particle velocity and the stress can be expressed as follows:

$$\{\overline{T}\} \equiv \begin{Bmatrix} \tau_{xx} \\ \tau_{yy} \\ \tau_{zz} \\ \tau_{xy} \\ \tau_{yz} \\ \tau_{zx} \end{Bmatrix} = \begin{bmatrix} \frac{4}{3}\mu\frac{\partial}{\partial x} & -\frac{2}{3}\mu\frac{\partial}{\partial y} & -\frac{2}{3}\mu\frac{\partial}{\partial z} \\ -\frac{2}{3}\mu\frac{\partial}{\partial x} & \frac{4}{3}\mu\frac{\partial}{\partial y} & -\frac{2}{3}\mu\frac{\partial}{\partial z} \\ -\frac{2}{3}\mu\frac{\partial}{\partial x} & -\frac{2}{3}\mu\frac{\partial}{\partial y} & \frac{4}{3}\mu\frac{\partial}{\partial z} \\ \mu\frac{\partial}{\partial y} & \mu\frac{\partial}{\partial x} & 0 \\ 0 & \mu\frac{\partial}{\partial z} & \mu\frac{\partial}{\partial y} \\ \mu\frac{\partial}{\partial z} & 0 & \mu\frac{\partial}{\partial x} \end{bmatrix} \begin{Bmatrix} \dot{u}_x \\ \dot{u}_y \\ \dot{u}_z \end{Bmatrix} \quad (4)$$

where $\dot{u}_x$, $\dot{u}_y$, and $\dot{u}_z$ are the particle velocities in the x, y, and z directions, respectively, at arbitrary points in the element, and μ is the coefficient of viscosity of the air. In the above equation, $\{\Gamma\}$ is the strain vector. The relationship between the particle velocity and the strain can be expressed by the constant strain element of a 3D tetrahedron as shown in Fig. 2.
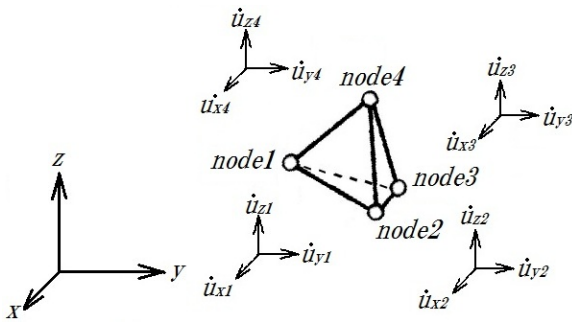

Fig. 2 Relationship between particle velocity and strain

$$\{\Gamma\} \equiv \begin{Bmatrix} \gamma_{xx} \\ \gamma_{yy} \\ \gamma_{zz} \\ \gamma_{xy} \\ \gamma_{yz} \\ \gamma_{zx} \end{Bmatrix} = \frac{1}{6V_e} \begin{bmatrix} b_1 & 0 & 0 & b_2 & 0 & 0 & b_3 & 0 & 0 & b_4 & 0 & 0 \\ 0 & c_1 & 0 & 0 & c_2 & 0 & 0 & c_3 & 0 & 0 & c_4 & 0 \\ 0 & 0 & d_1 & 0 & 0 & d_2 & 0 & 0 & d_3 & 0 & 0 & d_4 \\ c_1 & b_1 & 0 & c_2 & b_2 & 0 & c_3 & b_3 & 0 & c_4 & b_4 & 0 \\ 0 & d_1 & c_1 & 0 & d_2 & c_2 & 0 & d_3 & c_3 & 0 & d_4 & c_4 \\ d_1 & 0 & b_1 & d_2 & 0 & b_2 & d_3 & 0 & b_3 & d_4 & 0 & b_4 \end{bmatrix} \begin{Bmatrix} \dot{u}_{x1} \\ \dot{u}_{y1} \\ \dot{u}_{z1} \\ \dot{u}_{x2} \\ \dot{u}_{y2} \\ \dot{u}_{z2} \\ \dot{u}_{x3} \\ \dot{u}_{y3} \\ \dot{u}_{z3} \\ \dot{u}_{x4} \\ \dot{u}_{y4} \\ \dot{u}_{z4} \end{Bmatrix} \quad (5)$$

V_e is the volume of the element, and b_1–d_4 are constants. These constants can be expressed as follows:

$$\left. \begin{aligned} b_k &= \tilde{\varepsilon}_k \{ y_l(z_n - z_m) + y_m(z_l - z_n) + y_n(z_m - z_l) \} \\ c_k &= \tilde{\varepsilon}_k \{ z_l(x_n - x_m) + z_m(x_l - x_n) + z_n(x_m - x_l) \} \\ d_k &= \tilde{\varepsilon}_k \{ x_l(y_n - y_m) + x_m(y_l - y_n) + x_n(y_m - y_l) \} \\ \tilde{\varepsilon}_k &= \begin{cases} 1 & (k = 1,3) \\ -1 & (k = 2,4) \end{cases} \end{aligned} \right\} \quad (6)$$

where subscripts k, l, m, and n represent circular rotations of 1,

2, 3, and 4, respectively. Next, we consider the formulation of the motion equation of an element for the acoustic analysis model that considers viscous damping. The potential energy $\tilde{V}$ can be expressed as follows:

$$\tilde{V} = \int_\Gamma \{u\}^T \{\overline{P}\} d\Gamma + \iiint_e \{u\}^T \{F\} dxdydz \quad (7)$$

where $\{\overline{P}\}$ is the surface force vector, $\{F\}$ is the body force vector, and $\int_\Gamma d\Gamma$ represents the integral of the element boundary. The total energy $\tilde{E}$ can be derived by using the following expression:

$$\tilde{E} = \tilde{U} + \tilde{D} - \tilde{T} - \tilde{V} \quad (8)$$

We can obtain the following discretized equation of an element by using Lagrange's equations:

$$\frac{d}{dt}\frac{\partial \tilde{T}}{\partial \dot{u}_{ei}} - \frac{\partial \tilde{T}}{\partial u_{ei}} + \frac{\partial \tilde{U}}{\partial u_{ei}} - \frac{\partial \tilde{V}}{\partial u_{ei}} + \frac{\partial \tilde{D}}{\partial u_{ei}} = 0 \quad (9)$$

where u_{ei} is the ith component of the nodal displacement vector $\{u_e\}$, and $\dot{u}_{ei}$ is the ith component of the nodal particle velocity vector $\{\dot{u}_e\}$. We can obtain the following discretized equation of an element by substituting (1)–(7) into (9):

$$-\omega^2[M_e]\{u_e\} + [K_e]\{u_e\} + j\omega[C_e]\{u_e\} = \{f_e\} \quad (10)$$

We use $\{\dot{u}_e\} = j\omega\{u_e\}$ in this equation because a periodic motion having angular frequency ω is assumed. $[M_e]$, $[K_e]$, $[C_e]$, and $\{f_e\}$ are the element mass matrix, element stiffness matrix, element viscosity matrix, and nodal force vector, respectively.

III. CALCULATION

A. Damping Analysis by the Three-Dimensional Finite Element Method

To verify our method, we carried out an acoustic damping analysis for slits using 3D FEM. As shown in Fig. 3, this model is a 1/4 solid model symmetrical about the x-z plane and the x-y plane. The width of the model was 2.0mm, the height was 0.5mm, and the length was 16.6mm.
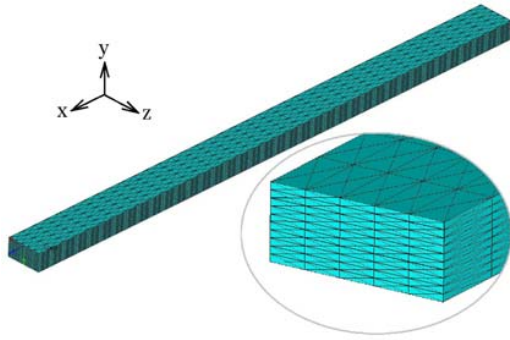
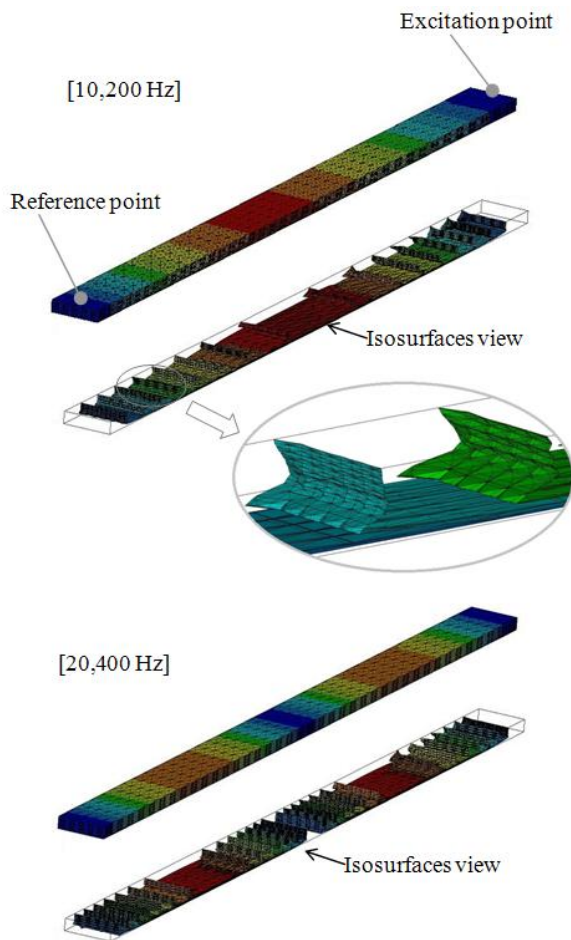Fig. 3 Three-dimensional slit model for the FEM

Fig. 4 The distribution of the particle displacement contour and the isosurface view (10,200Hz and 20,400Hz)

This model used 3D tetrahedral elements having four nodes. There were 39 divided elements in the length (x) direction, 10 layers in the height (y) direction and 5 layers in the width (z) direction. Both ends of this model were closed. We selected the effective density $\rho_R = 1.2$ kg/m^3, the coefficient of viscosity $\mu = 1.82 \times 10^{-5}$ N·s/m^2, the real part of the complex volume elasticity $E_R = 1.4 \times 10^5$ Pa, and the sound propagation speed c

= 340 m/s in air. As the boundary conditions, the particle displacements of all nodes on the outside in contact with surfaces were fixed, except for the plane of symmetry and the side walls which were not defined in the theoretical analysis. Fig. 4 shows the contours of the calculated particle displacements and the isosurface view of the model for the proposed finite element method, near the resonance conditions (10,200 Hz and 20,400 Hz). As can be seen, the magnitude of the displacement of the particles changes significantly near the contact surface. However, the displacement becomes flatter with distance from the contact surface.

B. Damping Analysis by Theoretical Analysis

We have carried out theoretical analysis of the resonant response of the slit to verify the proposed FEM. The frequency response of the pressure can be expressed by the following general expression [6]:

$$P = -j\rho c v_0 e^{j\omega t} \frac{\cos k(x-l)}{\sin kl} \qquad (11)$$

where ρ is density of the air, c is the speed of sound, l is the length of the slit, x is the position of a reference point, k is ω/c, v_0 is an excitation velocity, and t is time.
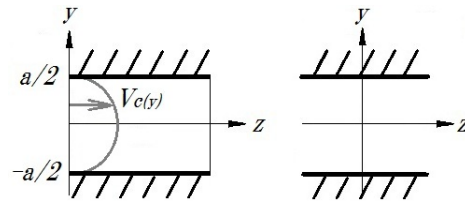
Fig. 5 The slit model and velocity $Vc_{(y)}$

In this equation, we introduce the complex sound speed c^* and the complex effective density ρ_c^* to include the attenuation due to the viscosity of the air. We replace the speed of sound and the density with the complex sound speed and the complex effective density as shown below.

$$\rho \Rightarrow \rho_c^* \qquad (12)$$

$$c \Rightarrow c^* \qquad (13)$$

Using the two substitutions above in (11) and the slit model is assumed infinite width, as shown in Fig. 5 the effective density can be expressed as follow [7]:

$$\rho_c^* = \frac{\rho_0}{1 - \dfrac{\tanh(s'j^{1/2})}{s'j^{1/2}}} \qquad (14)$$

where ρ_0 is mass density. s' and c^* are expressed as follow.

$$s' = \sqrt{\frac{\omega \rho_0 a^2}{\mu}} \qquad (15)$$

$$c^* = \sqrt{\frac{\kappa}{\rho_c^*}} = \sqrt{\frac{\gamma p_0}{\rho_c^*}} \qquad (16)$$

where a is the distance between the contact surfaces, κ is the bulk modulus, p_0 is atmospheric pressure, and γ is the specific heat at constant volume. For the case of $a = 0.5$mm, the complex density and complex sound velocity are shown in Figs. 6 and 7, respectively. By calculating the frequency response with (11) using the values of these parameters, the theoretical solution that includes the viscosity is obtained.
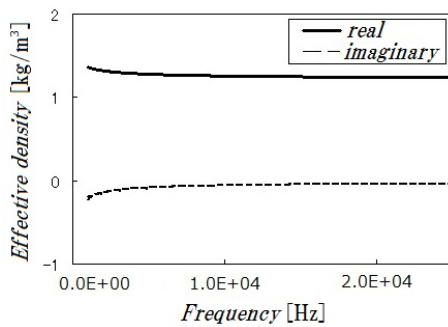

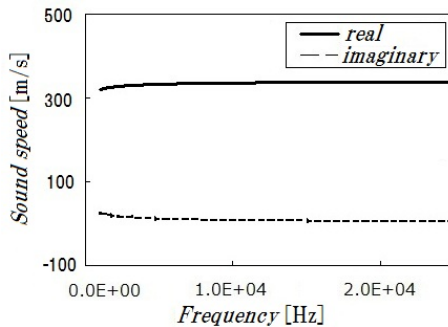Fig. 6 Effective density ρ_c^* in the slit model ($a = 0.5$mm)

Fig. 7 Sound speed c^* in the slit model (a=0.5mm)

C. Verification and Comparison of the Proposed Method

We have analyzed frequency responses using the proposed FEM, and compared them with the above-described theoretical method that includes the viscosity and with the conventional FEM that does not include the attenuation.

[a=0.8mm]
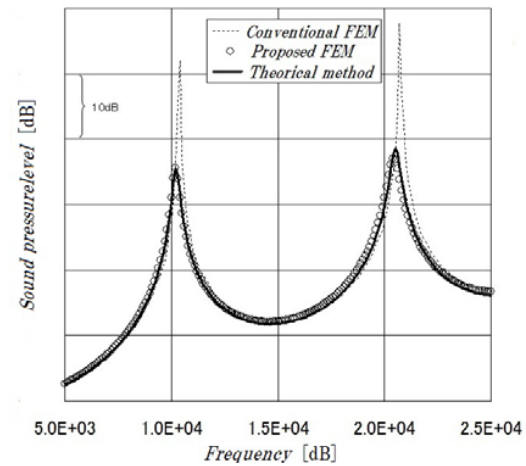
[a=0.50 mm]
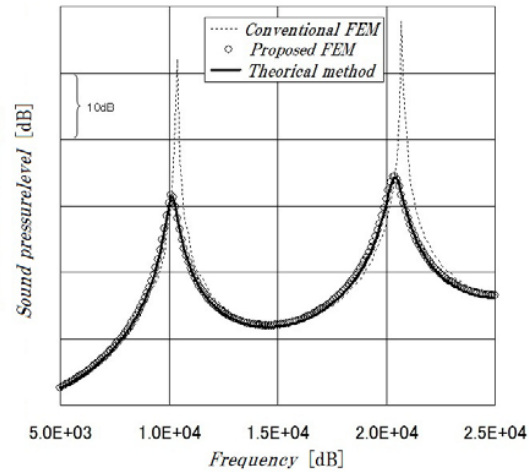
[a=0.25 mm]

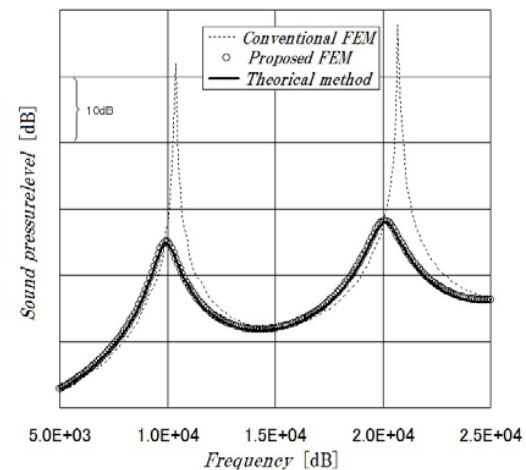
Fig. 8 Pressure versus frequency response for a slit model

Fig. 8 shows the comparison of the analysis results for models of $a = 0.8$, 0.5, 0.25mm. The condition of excitation

was constant displacement excitation. From Fig. 8, we determined the effect of damping on the calculated results by using the proposed FEM and the theoretical method. The conventional FEM does not show attenuation of the resonance peaks. As can be seen from Fig. 8, when the slit is narrow, the resonance peak decreases. That is, the attenuation increases when the slit width is narrowed. In addition, it can be seen that over the entire frequency domain, the calculated results of the proposed FEM and the theoretical method are approximately equal.

IV. CONCLUSION

We developed a new acoustic FEM that considers the effects of damping by the viscosity of air. We compared calculation results for sound pressure versus frequency characteristics using the proposed method with that of the theoretical method, and the conventional acoustic FEM without viscosity of air for slit models. The comparison showed that the calculated results are very close. Therefore, proposed new acoustic FEM was confirmed that have good analytic accuracy. We plan to consider the possibility of applying this analysis to various shapes in the future.

REFERENCES

[1] T. Yamaguchi, J. Tsugawa, H. Enomoto and Y. Kurosawa, "Layout of Sound Absorbing Materials in 3D Rooms Using Damping Contributions with Eigenvectors as Weight Coefficients," Journal of System Design and Dynamics, Vol. 4-1, pp. 166–176, 2010.
[2] T. Yamaguchi, Y. Kurosawa and H. Enomoto, "Damped Vibration Analysis Using Finite Element Method with Approximated Modal Damping for Automotive Double Walls with a Porous Material," Journal of Sound and Vibration, Vol. 325, pp. 436–450, 2009.
[3] M. Sasajima, T. Yamaguchi and A. Hara, "Acoustic Analysis Using Finite Element Method Considering Effects of Damping Caused by Air Viscosity in Audio Equipment," Applied Mechanics and Materials, Vol. 36, pp. 282–286, 2010.
[4] H. Utsuno, T. Tanaka, Y. Morisawa and T. Yoshimura, "Prediction of Normal Sound Absorption Coefficient for Multi-Layer Sound Absorbing Materials by Using the Boundary Element Method," Transactions of Japan Society of Mechanical Engineers, Vol. 56-532C, pp. 3248–3252, 1990.
[5] M. Sasajima, M. Watanabe, T. Yamaguchi, Y. Kurosawa, and Y. Koike," Acoustic Analysis with Consideration of Damping Effects of Air Viscosity in Sound Pathway," World Academy of science, Engineering and technology, ISSUE78,pp1011–1016, 2013.
[6] J.W. Strutt, B. Rayleigh, "The Theory of Sound (Second revised and enlarged edition)" New Yoke Dover Publications, Inc., pp54-57,1945.
[7] J.F. Allard, N. Atalla, "Propagation of Sound in Porous Media (Second Edition)" A John Wiley and Sons, Ltd., Publication, pp48–50, 2009.